

Geophysical Research Letters[®]

RESEARCH LETTER

10.1029/2024GL109282

Separating Common Signal From Proxy Noise in Tree Rings

M. Y. McPartland¹ , A. M. Dolman¹ , and T. Laepple^{1,2,3} 

¹Alfred-Wegener-Institut Helmholtz-Zentrum für Polar- und Meeresforschung, Research Unit Potsdam, Potsdam, Germany, ²MARUM—Center for Marine Environmental Sciences, University of Bremen, Bremen, Germany, ³Faculty of Geosciences, University of Bremen, Bremen, Germany

Key Points:

- Temperature-sensitive tree-ring records had the highest signal-to-noise ratios on an interannual basis
- Noise showed a positive relationship with timescale indicating presence of independent trends over long time periods
- Signal-to-noise ratios were highest in tree-ring density records and in records comprised of a greater number of individual trees

Supporting Information:

Supporting Information may be found in the online version of this article.

Correspondence to:

M. Y. McPartland,
mara.mcpartland@awi.de

Citation:

McPartland, M. Y., Dolman, A. M., & Laepple, T. (2024). Separating common signal from proxy noise in tree rings. *Geophysical Research Letters*, *51*, e2024GL109282. <https://doi.org/10.1029/2024GL109282>

Received 21 MAR 2024

Accepted 31 MAY 2024

Author Contributions:

Conceptualization: A. M. Dolman, T. Laepple

Data curation: M. Y. McPartland

Formal analysis: M. Y. McPartland, A. M. Dolman

Funding acquisition: T. Laepple

Investigation: M. Y. McPartland

Methodology: M. Y. McPartland, A. M. Dolman, T. Laepple

Project administration: M. Y. McPartland, T. Laepple

Resources: T. Laepple

Software: A. M. Dolman

Supervision: A. M. Dolman, T. Laepple

Writing – original draft: M. Y. McPartland

M. Y. McPartland

Abstract Tree rings are the most widely-used proxy records for reconstructing Common Era temperatures. Tree-ring records correlate strongly with temperature on an interannual basis, but studies have found discrepancies between tree rings and climate models on longer timescales, indicating that low-frequency noise could be prevalent in these archives. Using a large network of temperature-sensitive tree-ring records, we partition timeseries variance into a common (i.e., “signal”) and non-climatic (i.e., “noise”) component using a frequency-resolved signal-to-noise ratio (SNR) analysis. We find that the availability of stored resources from prior years (i.e., biological “memory”) dampens the climate signal at high-frequencies, and that independent noise reduces the SNR on long timescales. We also find that well-replicated, millennial-length records had the strongest common signal across centuries. Our work suggests that low-frequency noise models are appropriate for use in pseudoproxy experiments, and speaks to the continued value of high-quality data development as a top priority in dendroclimatology.

Plain Language Summary Tree rings contain valuable information about past variations in Earth's climate, but this information can be obscured by biological influences over tree-ring formation, particularly when slow changes in climate are integrated with long biological trends. In this study, we measured the strength of the common signal and random noise in a network of tree-ring records from across the Northern Hemisphere. We find that the emergence of non-climatic trends decreases the similarity of nearby tree-ring records to each other on long timescales.

1. Introduction

1.1. How Reliable Are Tree-Ring Records on Long Timescales?

Tree rings are rich paleoclimate archives that have been integral in reconstructing local to global-scale temperature variations over the last two millennia (Briffa et al., 2001, 2004; Esper et al., 2015; Mann et al., 2009; Neukom et al., 2019; PAGES, 2013; Wilson et al., 2016). On annual timescales, tree-ring records (also called “chronologies”) calibrate well with instrumental data, making them valuable records of high-frequency climate variations. However, the fidelity with which trees record the magnitude of medium- (decadal) and low-frequency (centennial and greater) climate variations is less evident.

Prior studies comparing tree rings to instrumental records and models disagree on whether reconstructions correctly represent long-term climate variability. For example, a number of reconstructions have shown that tree rings can produce variability on very long, even up to orbital timescales (Briffa et al., 2001; Esper et al., 2012; Klippel et al., 2020; Lücke et al., 2021; Wilson et al., 2016). However, Franke et al. (2013) found that tree-ring chronologies contain strong “red” biases on the lowest frequencies, indicating that they overrepresent variations on long timescales compared with instrumental and model data. Estimating the correct degree of long-term variability from models and data is challenging due to the limited period of the instrumental record, and because the strength of variability that should be expressed in climate models, particularly on the local scales experienced by trees, is debated (Deser et al., 2012; Laepple et al., 2023; Maher et al., 2020).

1.2. Multi-Temporal Influences Over Tree-Ring Formation

Tree rings integrate biological and ecological influences over annual ring formation with climate signals on all timescales (Cook, 1987; Fritts, 1976). On short (interannual) timescales, biological “memory” from prior years' growth modifies the in-year climate signal recorded during proxy formation such that timeseries are effectively smoothed across years (Matalas, 1962; Meko, 1981). Biological memory, caused by the carryover of stored

© 2024. The Author(s).

This is an open access article under the terms of the [Creative Commons Attribution-NonCommercial-NoDerivs License](#), which permits use and distribution in any medium, provided the original work is properly cited, the use is non-commercial and no modifications or adaptations are made.

Writing – review & editing:
M. Y. McPartland, A. M. Dolman,
T. Laepple

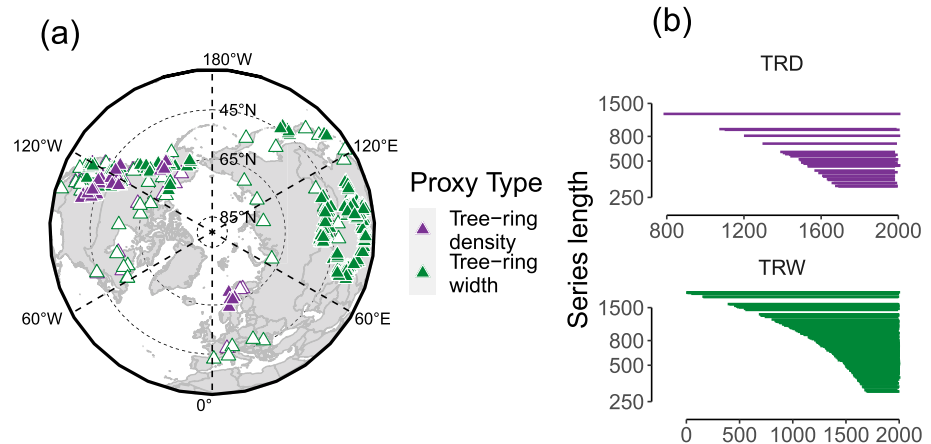


Figure 1. (a) Map of PAGES tree-ring sites included in analysis. White triangles are sites that did not meet the criteria to be included in the analysis either because they represented mixed proxy types or were too geographically isolated to be included in a cluster of <250 km radius, with a minimum of three sites represented. Density refers to both maximum latewood density and delta density chronologies. (b) Sample density plot showing the series length of each chronology.

resources from one year to the next, is known to lengthen the proxy response to extreme cooling events such as volcanoes, and has been identified as one source of discrepancy between annual ring-width data and instrumental records on short timescales (Esper et al., 2015; Lücke et al., 2019; Zhang et al., 2015; Zhu et al., 2020).

On longer (decadal and greater) timescales, a number of non-climate factors can influence tree growth. For example, any stand-wide disturbance event that affects growth among a majority of trees within a chronology will result in the presence of a shared trend of varying length (Cook, 1985, 1987). In addition, in the early stage of development, juvenile trees typically create wide rings of less-dense wood as the tree devotes resources to rapid growth, such that the early part of tree-ring chronologies are dominated by age effects (Fritts, 1976). In order to remove these biological trends, “detrending” is a near universal step in tree-ring data development. This involves transforming the individual, raw data against data-adaptive spline or low-pass filter functions that model the age-dependence of tree-ring formation. Removing the age-growth trend from tree-ring records can also remove low-frequency climate information (Cook & Kairiukstis, 1990; Cook & Peters, 1997; Cook et al., 1995), although some methods attempt to recover or retain shared variance during detrending (Esper et al., 2003; Melvin & Briffa, 2008, 2014a, 2014b). Despite detrending, it is likely that some non-climatic trends are propagated through to final chronologies, especially in cases where the detrending method is intended to retain low-frequency variability.

1.3. Estimation of Timescale-Dependent Signal-To-Noise Ratios

Here, we offer a systematic evaluation of timescale-dependent common signal-to-noise ratios in temperature sensitive tree-ring records. This straightforward method estimates shared signal and independent noise in regional clusters of records as a function of timescale (Münch & Laepple, 2018). This approach avoids direct comparisons with models or instrumental data by leveraging the regional climate signal that should be reflected in sites at close proximity, relative to the decorrelation length of temperature variations. Our work addresses outstanding questions regarding the nature of low-frequency variability in tree-ring records for the purpose of correctly estimating the magnitude of past temperature variations.

2. Data

2.1. Northern Hemisphere Tree-Ring Network

This study analyzes the Past Global Changes (PAGES) 2K database, a global multi-proxy network of 647 unique temperature-sensitive paleoclimate time series, including 450 tree-ring timeseries (Figure 1a) (PAGES 2k Consortium et al., 2013; PAGES 2k Consortium et al., 2017; Neukom et al., 2019). For this analysis, we used all Northern Hemisphere records, with the greatest density of sites located in central Asia and western North America (Figure 1a). We opted to exclude Southern Hemisphere sites because fewer sites are located there, and because

our analysis relied on sample density. The PAGES network includes both total ring width (TRW), and tree-ring density (TRD) records. These are mainly maximum latewood density records, with a small number of records of delta density (i.e., the difference between early and latewood density) (Björklund et al., 2014; Linderholm et al., 2015). For this study, we analyzed ring width and density records independently for comparison among proxy types. The vast majority of sites within the PAGES database were detrended with negative exponential curves, although Arctic and European sites were detrended using regional curve standardization (PAGES 2k Consortium et al., 2013; PAGES 2k Consortium et al., 2017).

In addition, we used a more extensive version of the PAGES North America (NAM2k) database ($n = 290$) that was used to develop the global database. The NAM2k database contains additional chronologies, some of which were not included in final the global database, with versions of each chronology detrended in six different ways (Figure S1 in Supporting Information S1). The expanded database also includes additional metadata, such as the number of individual tree cores contributing to the chronology at each timestep. We exploited this more extensive set of records to look at the relationship between within-chronology replication and the effects of detrending on SNR (Figure S1 in Supporting Information S1).

3. Methods

3.1. Spatial Clustering of Sites for Signal-To-Noise Ratio Estimation

Our method relies on the assumption that all sites within a cluster experienced the same variations in climate. The spatial decorrelation length of Northern Hemisphere temperatures is roughly 1,000–3,000-km on an interannual basis (Hansen & Lebedeff, 1987; North et al., 2011), so we defined a conservative radius of 250-km such that the furthest distance any two sites could be apart was 500 km. We implemented a clustering method based on a Euclidian distance matrix organized such that a single site could be present in multiple clusters. Clusters were filtered to contain at minimum three sites per cluster in order to optimize between cluster size and the density of sites per cluster. While defining a larger cluster size would result in a greater replication, it also risks shifting some climate related variance into the noise fraction as the climate becomes less coherent at large spatial scales. The spatial clustering scheme resulted in 253 clusters globally: 18 clusters of TRD sites and 235 clusters of TRW sites. We additionally analyzed a subset of clusters where every chronology represented in the cluster was over 800 years in length, in order to determine the effects of chronology length. Only eight tree-ring width clusters met this criterion.

The vast majority (421 out of 450) records in the PAGES database were included in our analysis and the same record could appear in multiple clusters. The remainder were too spatially isolated to meet the criteria (<500 km from at least two other sites) (Figure 1a). The average length of the overlapping period among sites in a cluster was 451 years, and the average number of sites per cluster was eight. For the NAM2k database, 29 density clusters and 157 tree-ring width clusters were analyzed with an average overlapping period of 348 years and an average of nine sites per cluster.

3.2. Statistical Approach

We estimated timescale dependent signal and noise components in the spectral domain using the methodology developed by Münch and Laepple (2018), similar to an analysis of variance. Assuming the noise is independent between records, but the signal is the same, the noise (N_f) is estimated by taking the spectra of all series averaged in the time domain (C_f), which contains the shared signal (S_f) but with reduced noise as a result of averaging. This noise term is then subtracted it from the mean of all individual spectra (M_f), an estimate which should contain both the signal and full noise:

$$\text{Spectra of mean time series : } C_f = S_f + \frac{N_f}{n}$$

$$\text{Mean of all spectra : } M_f = S_f + N_f$$

The greater the replication in the stack, the more the noise is reduced. Thus, the noise term is estimated as:

$$N_f = \frac{M_f - C_f}{1 - \frac{1}{n}}$$

The common signal is then the difference between mean of all spectra and the noise term:

$$S_f = M_f - N_f$$

In which case, the SNR is the ratio of the signal and noise:

$$\text{SNR}_f = \frac{S_f}{N_f}$$

These estimates were averaged together across clusters to evaluate how well both proxies perform at retaining shared climate signal on all timescales. All spectra were computed using the multi-taper spectral estimate, and spectral slopes (β) were calculated as the linear relationship between frequency and power on a log-log scale to describe the shape of the spectrum (Thomson, 1982). We note here that our signal-to-noise ratio estimation is based on chronology variance as in Fisher et al. (1985) rather than standard deviation, which has been used in some studies (Mann et al., 2007; Smeardon, 2012; Zhu et al., 2023). This is because power spectral density is expressed in variance per frequency unit, and is thus more common in signal processing (Jenkins & Priestley, 1957).

Confidence limits were calculated for our estimates using parametric bootstrapping (Nelson, 2008). Stochastic timeseries were simulated such as to have power-law scaling spectra with the same variance (α) and spectral slope (β) as the original tree-ring data, with the same mean length and number of series per cluster, effectively preserving the structure of the analysis. One thousand iterations were run over each cluster. Signal, noise and SNR were calculated for each iteration (set of simulated data) and confidence limits were estimated as the 10th and 90th percentiles across iterations (Text S1 in Supporting Information S1). Spectral estimates were truncated at 1/100-year timescales due to the drop in sample density after that time period. Multi-centennial timescales were only achieved in the longest TRW records, which were analyzed separately.

We compared the raw and corrected signal spectral estimates to instrumental data to determine how well tree rings reproduce the shape of the power spectra represented in observational temperature records. We used the infilled version of the HadCRUT5 $5 \times 5^\circ$ temperature anomaly data set calculated on a 1961–1990 reference baseline for the 1850–2020 period (Morice et al., 2021). HadCRUT grid cells were extracted nearest to each point, removing duplicate records where multiple tree-ring sites shared the same pixel. Individual spectra were calculated for all instrumental time series, and averaged to get a the mean spectra of temperature. Confidence intervals were calculated assuming 10 degrees of freedom as a conservative estimate of the number of independent spatial climate modes at these timescales (Kunz & Laepple, 2024).

To investigate the effect of biological memory, we estimated the smoothing filter that would be required to adjust the corrected tree-ring spectra to match the slope of the HadCRUT spectrum. To do this we assumed a negative exponential filter in the time domain acting only on past values (past but not future climate can affect this year's growth). Using the HadCRUT spectra as the reference, we fitted the negative exponential filter to the ratio of the tree ring to climate spectra by adjusting the timescale of the filter. This estimated how much additional smoothing would be required to adjust the tree-ring data to match the spectral properties of the HadCRUT data. This yielded an estimate of the effect of any given year of growth on subsequent years. We did this for the uncorrected (“raw”) spectrum and the corrected version for both TRD and TRW.

We also estimated the Partial Autocorrelation Function (PACF) of the HadCRUT, raw and corrected tree-ring spectra. We did this by creating simulated timeseries with the same spectral properties and then use these simulations to estimate the PACF of tree rings and climate data at lagged years 1–4. One hundred simulated timeseries were calculated for each tree-ring proxy type, for raw, corrected and HadCRUT and the average first-through forth-order mean PACF were calculated from this sample.

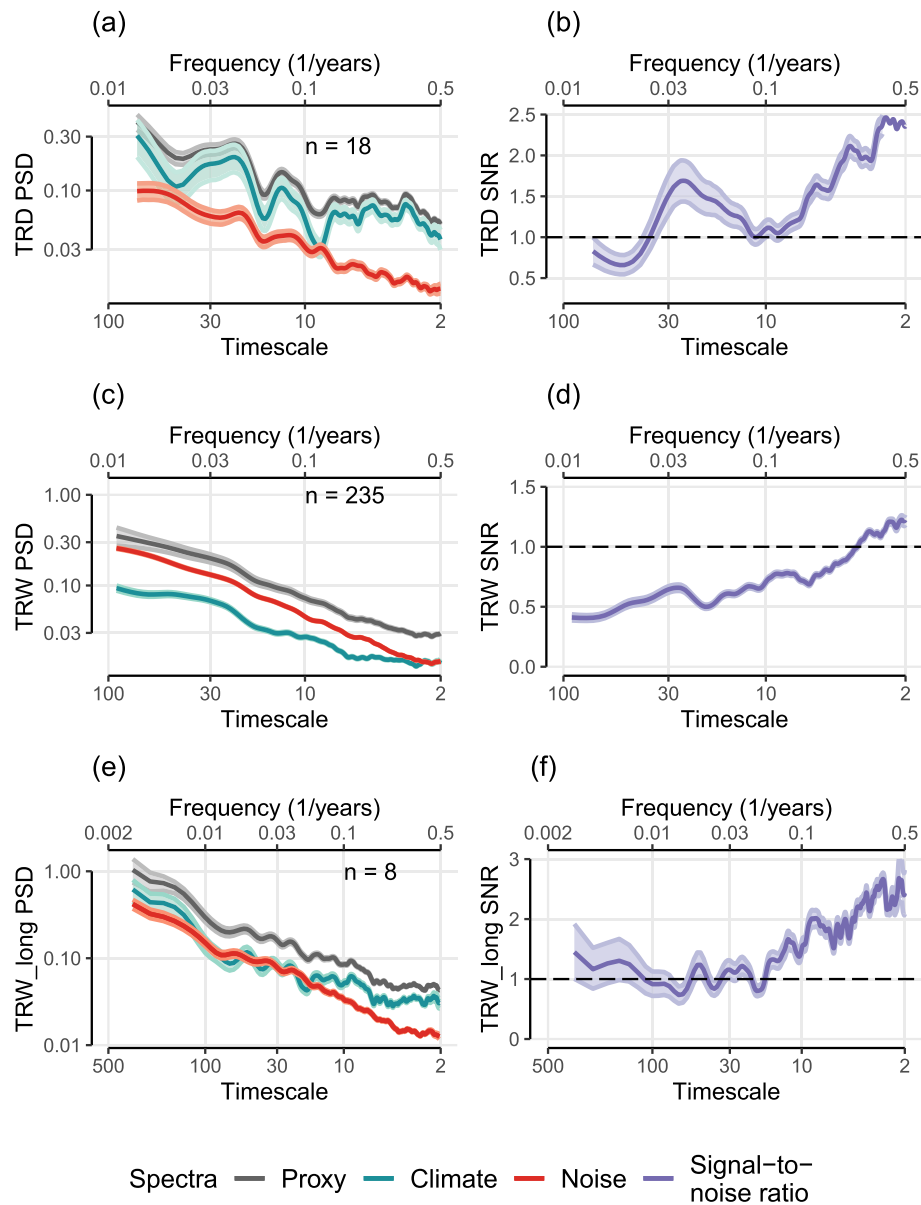


Figure 2. Left panels—Comparison of uncorrected proxy, common climate signal, and noise spectra for (a) density, (c) tree-ring width and (e) tree-ring width exceeding 800 years in length. Right panels—Signal-to-noise ratio estimates for (b) density, (d) tree-ring width, and (f) tree-ring width series exceeding 800 years in length. Confidence intervals represent the 10th and the 90th percentiles from the parametric bootstrapping estimation. Note that the confidence intervals in subplots (c) and (d) have confidence intervals very close to the line due to the high level of replication.

4. Results

4.1. Timescale Dependent Signal, Noise and SNR Spectral Estimates

Our result showed that the power-spectra of both TRW and TRD records, for the signal and noise spectra have spectral slopes (β) between 0.5 and 1 (Figure 2). The β of the noise spectrum for TRW was 0.83 for all records (Figure 2c), and $\beta = 0.70$ for the longest TRW records (Figure 2e). For TRD records, the spectrum of the noise had a β of 0.58 (Figure 2a).

We found that the SNR for both proxy types was highest on interannual timescales and declined into the multi-decadal (Figures 2b, 2d, and 2f). TRD had nearly double the SNR as TRW on all timescales. For all TRW records,

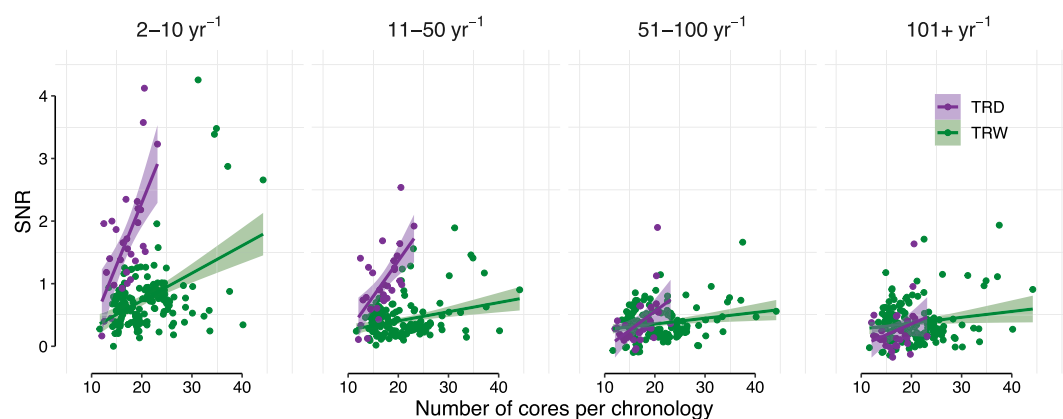


Figure 3. Relationship between mean number of cores per chronology contained in each cluster, and the resulting signal-to-noise ratio of the cluster, binned by frequency and fitted with linear regression lines with one standard error indicated by the shaded region.

the SNR was at slightly above one at two-to-five years, and declined to 0.5 after around 8 years, and then was relatively flat. TRD maintained an SNR of two until around 10 years and then maintained around an SNR of one into multidecadal timescales. There was a slight increase in TRD SNR around 30 years, possibly due to the stronger expression of variability at those locations and timescales (Figure 2b). The longest TRW records (all with records of at least 800 years), behaved more similarly to TRD with an SNR of two until around 20 years, and then a ratio of one into multi-centennial timescales (Figure 2f).

4.2. Chronology Sample Density and SNR

We found a positive relationship between the average number of cores per chronology and SNR (Figure 3). This relationship was stronger for TRD than TRW records (TRD had an overall higher SNR), and it was highest for both proxy types in the interannual to decadal band (2–10 years). The strength of the effect of core number declined with timescale along with the overall SNR for both proxy types.

4.3. Comparison of Corrected Spectra to the Instrumental Record

A comparison of spectral slopes (β) of the raw and corrected signal showed that correction brought both TRW and TRD slopes into better alignment with that of HadCRUT ($\beta = 0.31$). The corrected TRW and TRD spectra had β values of 0.53 and 0.38, respectively, down from 0.72 to 0.40 before correction, hence a larger discrepancy remained for TRW than for TRD.

While the shape of the corrected TRD curve matched that of instrumental record across all frequencies, the TRW spectrum showed significantly reduced variability on interannual timescales (Figure 4a). The quantification of biological memory yielded a value of 0.13, for lagged year one, indicating a 13% dependency of any given years' value on the previous year, decaying toward zero after three years following an exponential model (Figure 4b). TRD exhibited far less dependency across, with only a 4% dependency after one year, decreasing to near zero at year two. To compare our results to previous estimates of PACF in tree rings, we simulated timeseries with the same spectral properties as the uncorrected spectrum and find that our results were consistent to prior research (Lücke et al., 2019). After noise removal, PACF coefficients were smaller indicating that the earlier estimates were biased by site-specific noise. However, at lag 1, PACF coefficients remained relatively larger for TRW compared with TRD and HadCRUT, consistent with a memory effect on TRW in particular (Esper et al., 2015; Lücke et al., 2019; Zhang et al., 2015; Zhu et al., 2020). Any differences in PACF among records decayed to around zero after three years (Figure 4c).

5. Discussion

By analyzing clustered records within close proximity we systematically estimate timescale-dependent common variance and independent noise without referring to model or instrumental data. By doing this we do not rely on

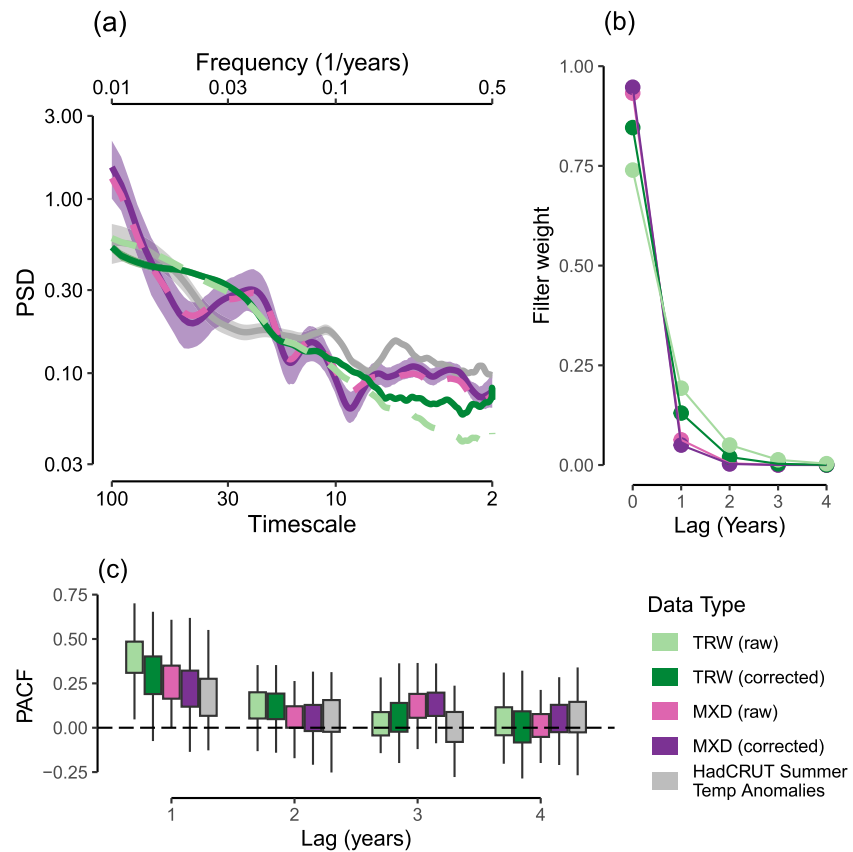


Figure 4. (a) Comparison of mean “corrected” climate signal spectra from tree-ring with and density chronologies, with the Hadley Climate Research Unit Climate time series (HadCRUT). All spectra have been scaled to have the same mean power spectral density on 8–100 year timescales to demonstrate the spectral discrepancy in the high frequencies. (b) Estimation of filter response function for each tree-ring spectra compared with HadCRUT data. (c) Partial autocorrelation coefficients (PACF) measured on simulated time series generated using raw and corrected spectral estimates, for one to four year lags.

short instrumental records for long-term information, and avoid questions regarding potential low-frequency biases in climate models (Cheung et al., 2017; Fredriksen & Rypdal, 2016; Hébert et al., 2022; Laepple & Huybers, 2014; Laepple et al., 2023; Zhu et al., 2019). Using a simple analytical approach we show that large low-frequency (i.e., “red”) noise is ubiquitous across dendrochronology archives, even in highly-temperature sensitive chronologies, consistent with the findings from Franke et al. (2013). Our results indicate that tree-ring density records contained nearly double the signal-to-noise ratio compared with tree-ring width, also unsurprising given that density is considered the better proxy for temperature. Our findings deepen an existing understanding within dendrochronology regarding the integration of climatic and non-climatic signals on all timescales. These results can be used to guide new chronology development and can be applied within pseudoproxy experimentation to accurately model the structure of proxy noise.

5.1. Sources of Proxy Noise in Tree-Ring Records on Slow and Fast Timescales

There are multiple possible sources of medium- and low-frequency noise that may affect tree-ring chronologies. Noise may be caused by differences in site-level environmental conditions, the mixing of climatic constraints on tree growth, or by stand-wide disturbances. For example, an extreme but local climatic event such as a major storm, or an outbreak of a pest or pathogen that affects the majority of trees within a stand could result in a multi-decadal recovery trend (Foster, 1988; Pederson et al., 2014; Rydval et al., 2016). It is also possible that local climatic differences could cause independent variance at the site-level that would be mischaracterized as noise by our method. While the PAGES database was curated to maximize temperature-sensitivity, some sites might be limited by precipitation as well as temperature, or could be sensitive to temperature within different parts of the growing season (St. George & Ault, 2014; Tardif et al., 2019; Zhu et al., 2020). The combination of local

environmental and climate conditions, and ecological interactions all could create emergent trends that become integrated with slow climate variations (Cook, 1985; Cook & Kairiukstis, 2010).

Low-frequency noise could also be an artifact of the detrending process imperfectly removing age-growth trends or distorting the shared signal on long timescales (Cook & Peters, 1997; Helama et al., 2004; Melvin & Briffa, 2008). The “divergence phenomenon”—the observation that the correlation strength between temperature records and tree growth appeared to diminish after the 1980s—was posited to be a result of detrending resulting in the distortion of growth trends, particularly at the ends of chronologies (Cook & Peters, 1997; D’Arrigo et al., 2008; Esper & Frank, 2009; Melvin & Briffa, 2008). This led to the introduction of several new detrending methods, including “signal-free detrending” aimed at improving the expression of common low-frequency climate signal while avoiding trend distortion (Melvin & Briffa, 2008). In a supplementary analysis of four different detrending techniques, we found that detrending method didn’t meaningfully change the SNR (Figure S2 in Supporting Information S1). Signal-free detrending did result in a slight increase in chronology SNR at long timescales, consistent with the results of McPartland et al. (2020), but the effect was small. That detrending didn’t make a large difference is evidence that red noise is either non-climatic, or represents site-level but not regional climate conditions.

Having removed independent noise at high frequencies, we were able to estimate biological memory through comparison with the instrumental record. We show both that this memory lasts on average one to two years, and is of a magnitude consistent with the findings of other studies (Esper et al., 2015; Lücke et al., 2019; Zhang et al., 2015). Unlike in the case of low-frequency variability, the autocorrelation structure of temperature records can be estimated directly from instrumental data, and tree rings can be adjusted to the climate using autoregressive modeling (Meko, 1981).

5.2. Possibilities for Recovering Low-Frequency Climate Signals From Tree Rings

We show that the fraction of shared signal drops precipitously as fewer individual trees contribute to site-level and regional estimates. In a small subset of chronologies where all records in a given cluster reached over 800 years in length, the SNR remained higher into multi-centennial timescales. This result speaks to the fundamental challenge of recovering climate variations that occur over longer than the typical lifespan of a tree—a constraint known as the “segment length curse” (Cook et al., 1995). This age-related constraint is exacerbated by the detrending process that inevitably removes some low-frequency climate variability (Briffa et al., 1996; Cook, 1985). The converse problem is also expected—that even as low-frequency climate information could be removed during detrending, some influence of life history will remain in final chronologies.

Our results suggest that long chronology length and high sample replication boost the climate signal strength on multi-centennial timescales. This is a main tenant of dendrochronology—that replication is key to improving chronology quality (Speer, 2010). We find that SNR was positively correlated with sample density, such that more cores extending to longer timescales resulted in a significantly stronger signal strength. This suggests that the value of extending a chronology back in time using a single or very few records is likely small as low sample density will result in increased noise. Such samples and sites are rare, but our results underscore that developing millennial-length records continues to be a priority for estimating the long-term behavior of the global climate system.

5.3. Application of Red Noise Models in Pseudoproxy Experiments

Our results address the question of how to correctly define the structure of the noise term in pseudoproxy experiments and data assimilation frameworks where proxy timeseries are integrated with climate models (Dee et al., 2017; Jones et al., 2009; Smeardon, 2012; Steiger et al., 2014). In past such experiments, a variety of different noise models have been used ranging from blue (i.e., noise that diminishes with timescale) (Mann & Rutherford, 2002; Mann et al., 2007), to white (i.e., no relationship to timescale) (Lee et al., 2008; Mann et al., 2005; Von Storch et al., 2004) to red (noise that increases with timescale) (Von Storch et al., 2009; Zhu et al., 2023). Here, we estimate the structure of proxy noise directly from the data and show that noise in tree-ring width records resembles a power-law (slope of 0.8), and in tree-ring density records exhibit a less-steep positive noise spectrum (slope of 0.5–0.6). We suggest that red noise models best describe the behavior of both tree-ring width and density data. Our findings can be applied directly to the creation of tree-ring pseudoproxy timeseries, allowing for an improved evaluation of the performance of models and reconstructions on all timescales.

Conflict of Interest

The authors declare no conflicts of interest relevant to this study.

Data Availability Statement

The main PAGES2k (PAGES2k Consortium et al., 2017) and North American PAGES detrended databases are publicly-available through the NOAA National Centers for Environmental Information (Anchukaitis et al., 2024; Emile-Geay et al., 2017). The Hadley Climate Research Unit Time Series Version 5 data set is available on the HadCRUT website (Morice et al., 2021). The code needed to reproduce this analysis is archived in Zenodo (McPartland, 2024).

Acknowledgments

This is a contribution to the SPACE ERC project; this project has received funding from the European Research Council (ERC) under the European Union's Horizon 2020 research and innovation program (Grant Agreement 716092). A. Dolman was supported by the Deutsche Forschungsgemeinschaft (DFG, German Research Foundation)—Project number 468685498 (A.M.D.)—SPP 2299/Project number 441832482. Funding to compile the PAGES NAM2K data set was originally provided by the USGS Powell Center for Synthesis and Analysis. We acknowledge support from the Open Access Publication Funds of Alfred-Wegener-Institut Helmholtz-Zentrum für Polar- und Meeresforschung. We also acknowledge the contributions of Dr. Raphaël Hébert and members of the AWI-Earth System Diagnostics Group. Thanks also to Drs. Kevin Anchukaitis, Nick McKay, Cody Routson, Scott St. George, Uday Thapa, and Greg Pederson for help with data archiving. Open Access funding enabled and organized by Projekt DEAL.

References

- Anchukaitis, K. J., Pederson, G. T., St. George, S., McKay, N. P., Routson, C., & Thapa, U. K. (2024). PAGES North America 2k detrending database [Dataset]. NOAA National Centers for Environmental Information. Retrieved from <https://www.nccei.noaa.gov/access/paleo-search/study/39559>
- Björklund, J. A., Gunnarson, B. E., Seftigen, K., Esper, J., & Linderholm, H. W. (2014). Blue intensity and density from northern Fennoscandian tree rings, exploring the potential to improve summer temperature reconstructions with earlywood information. *Climate of the Past*, 10(2), 877–885. <https://doi.org/10.5194/cp-10-877-2014>
- Briffa, K. R., Jones, P. D., Schweingruber, F. H., Karlén, W., & Shiyatov, S. G. (1996). Tree-ring variables as proxy-climate indicators: Problems with low-frequency signals. In P. D. Jones, R. S. Bradley, & J. Jouzel (Eds.), *Climatic variations and forcing mechanisms of the last 2000 years* (pp. 9–41). Springer. https://doi.org/10.1007/978-3-642-61113-1_2
- Briffa, K. R., Osborn, T. J., & Schweingruber, F. H. (2004). Large-scale temperature inferences from tree rings: A review. *Global and Planetary Change*, 40(1), 11–26. [https://doi.org/10.1016/S0921-8181\(03\)00095-X](https://doi.org/10.1016/S0921-8181(03)00095-X)
- Briffa, K. R., Osborn, T. J., Schweingruber, F. H., Harris, I. C., Jones, P. D., Shiyatov, S. G., & Vaganov, E. A. (2001). Low-frequency temperature variations from a northern tree ring density network. *Journal of Geophysical Research*, 106(D3), 2929–2941. <https://doi.org/10.1029/2000JD900617>
- Cheung, A. H., Mann, M. E., Steinman, B. A., Frankcombe, L. M., England, M. H., & Miller, S. K. (2017). Comparison of low-frequency internal climate variability in CMIP5 models and observations. *Journal of Climate*, 30(12), 4763–4776. <https://doi.org/10.1175/JCLI-D-16-0712.1>
- Cook, E. R. (1985). A time series analysis approach to tree ring standardization. Retrieved from <https://www.st-andrews.ac.uk/~rjsw/PalaeoPDFs/Cook1985-Chapter%202.pdf>
- Cook, E. R. (1987). The decomposition of tree-ring series for environmental studies. *Tree-Ring Bulletin*. Retrieved from <https://repository.arizona.edu/handle/10150/261788?show=full>
- Cook, E. R., Briffa, K. R., Meko, D. M., Graybill, D. A., & Funkhouser, G. (1995). The “segment length curse” in long tree-ring chronology development for palaeoclimatic studies. *The Holocene*, 5(2), 229–237. <https://doi.org/10.1177/095968369500500211>
- Cook, E. R., & Kairiukstis, L. A. (1990). *Methods of dendrochronology: Applications in the environmental sciences*. Springer Science & Business Media.
- Cook, E. R., & Peters, K. (1997). Calculating unbiased tree-ring indices for the study of climatic and environmental change. *The Holocene*, 7(3), 361–370. <https://doi.org/10.1177/095968369700700314>
- D'Arrigo, R., Wilson, R., Liepert, B., & Cherubini, P. (2008). On the ‘divergence problem’ in northern forests: A review of the tree-ring evidence and possible causes. *Global and Planetary Change*, 60(3), 289–305. <https://doi.org/10.1016/j.gloplacha.2007.03.004>
- Dee, S. G., Parsons, L. A., Loope, G. R., Overpeck, J. T., Ault, T. R., & Emile-Geay, J. (2017). Improved spectral comparisons of paleoclimate models and observations via proxy system modeling: Implications for multi-decadal variability. *Earth and Planetary Science Letters*, 476, 34–46. <https://doi.org/10.1016/j.epsl.2017.07.036>
- Deser, C., Phillips, A., Bourdette, V., & Teng, H. (2012). Uncertainty in climate change projections: The role of internal variability. *Climate Dynamics*, 38(3), 527–546. <https://doi.org/10.1007/s00382-010-0977-x>
- Emile-Geay, J., McKay, N. P., Kaufman, D. S., von Gunten, L., Wang, J., Anchukaitis, K. J., et al. (2017). NOAA/WDS paleoclimatology - PAGES2k global 2,000 year multiproxy database [Dataset]. NCIE. <https://doi.org/10.25921/YCR3-7588>
- Esper, J., Cook, E. R., Krusic, P. J., Peters, K., & Schweingruber, F. H. (2003). Tests of the RCS method for preserving low-frequency variability in long tree-ring chronologies. Retrieved from <https://repository.arizona.edu/handle/10150/262573>
- Esper, J., & Frank, D. (2009). Divergence pitfalls in tree-ring research. *Climatic Change*, 94(3–4), 261–266. <https://doi.org/10.1007/s10584-009-9594-2>
- Esper, J., Frank, D. C., Timonen, M., Zorita, E., Wilson, R. J. S., Luterbacher, J., et al. (2012). Orbital forcing of tree-ring data. *Nature Climate Change*, 2(12), 862–866. <https://doi.org/10.1038/nclimate1589>
- Esper, J., Schneider, L., Smerdon, J. E., Schöne, B. R., & Büntgen, U. (2015). Signals and memory in tree-ring width and density data. *Dendrochronologia*, 35, 62–70. <https://doi.org/10.1016/j.dendro.2015.07.001>
- Fisher, D. A., Reeh, N., & Clausen, H. B. (1985). Stratigraphic noise in time series derived from ice cores. *Annals of Glaciology*, 7, 76–83. <https://doi.org/10.3189/S0260305500005942>
- Foster, D. R. (1988). Disturbance history, community organization and vegetation dynamics of the old-growth Pisgah forest, South-Western New Hampshire, U.S.A. *Journal of Ecology*, 76(1), 105–134. <https://doi.org/10.2307/2260457>
- Franke, J., Frank, D., Raible, C. C., Esper, J., & Brönnimann, S. (2013). Spectral biases in tree-ring climate proxies. *Nature Climate Change*, 3(4), 360–364. <https://doi.org/10.1038/nclimate1816>
- Fredriksen, H.-B., & Rypdal, K. (2016). Spectral characteristics of instrumental and climate model surface temperatures. *Journal of Climate*, 29(4), 1253–1268. <https://doi.org/10.1175/JCLI-D-15-0457.1>
- Fritts, H. (1976). *Tree rings and climate*. Elsevier.
- Hansen, J., & Lebedeff, S. (1987). Global trends of measured surface air temperature. *Journal of Geophysical Research*, 92(D11), 13345–13372. <https://doi.org/10.1029/JD092iD11p13345>

- Hébert, R., Herzschuh, U., & Laepple, T. (2022). Millennial-scale climate variability over land overprinted by ocean temperature fluctuations. *Nature Geoscience*, *15*(11), 899–905. <https://doi.org/10.1038/s41561-022-01056-4>
- Helama, S., Lindholm, M., Timonen, M., & Eronen, M. (2004). Detection of climate signal in dendrochronological data analysis: A comparison of tree-ring standardization methods. *Theoretical and Applied Climatology*, *79*(3), 239–254. <https://doi.org/10.1007/s00704-004-0077-0>
- Jenkins, G. M., & Priestley, M. B. (1957). The Spectral Analysis of Time-Series. *Journal of the Royal Statistical Society: Series B*, *19*(1), 1–12. <https://doi.org/10.1111/j.2517-6161.1957.tb00240.x>
- Jones, P. D., Briffa, K. R., Osborn, T. J., Lough, J. M., van Ommen, T. D., Vinther, B. M., et al. (2009). High-resolution palaeoclimatology of the last millennium: A review of current status and future prospects. *The Holocene*, *19*(1), 3–49. <https://doi.org/10.1177/0959683608098952>
- Klippel, L., St. George, S., Büntgen, U., Krusic, P. J., & Esper, J. (2020). Differing pre-industrial cooling trends between tree rings and lower-resolution temperature proxies. *Climate of the Past*, *16*(2), 729–742. <https://doi.org/10.5194/cp-16-729-2020>
- Kunz, T., & Laepple, T. (2024). Effective spatial degrees of freedom of natural temperature variability as a function of frequency. *Journal of Climate*, *1*(aop), 2505–2518. <https://doi.org/10.1175/JCLI-D-23-0040.1>
- Laepple, T., & Huybers, P. (2014). Ocean surface temperature variability: Large model–data differences at decadal and longer periods. *Proceedings of the National Academy of Sciences*, *111*(47), 16682–16687. <https://doi.org/10.1073/pnas.1412077111>
- Laepple, T., Ziegler, E., Weitzel, N., Hébert, R., Ellerhoff, B., Schoch, P., et al. (2023). Regional but not global temperature variability underestimated by climate models at supradecadal timescales. *Nature Geoscience*, *16*(11), 958–966. <https://doi.org/10.1038/s41561-023-01299-9>
- Lee, T. C. K., Zwiers, F. W., & Tsao, M. (2008). Evaluation of proxy-based millennial reconstruction methods. *Climate Dynamics*, *31*(2), 263–281. <https://doi.org/10.1007/s00382-007-0351-9>
- Linderholm, H. W., Björklund, J., Seftigen, K., Gunnarson, B. E., & Fuentes, M. (2015). Fennoscandia revisited: A spatially improved tree-ring reconstruction of summer temperatures for the last 900 years. *Climate Dynamics*, *45*(3), 933–947. <https://doi.org/10.1007/s00382-014-2328-9>
- Lücke, L. J., Hegerl, G. C., Schurer, A. P., & Wilson, R. (2019). Effects of Memory Biases on Variability of Temperature Reconstructions. *Journal of Climate*, *32*(24), 8713–8731. <https://doi.org/10.1175/JCLI-D-19-0184.1>
- Lücke, L. J., Schurer, A. P., Wilson, R., & Hegerl, G. C. (2021). Orbital forcing strongly influences seasonal temperature trends during the last millennium. *Geophysical Research Letters*, *48*(4), e2020GL088776. <https://doi.org/10.1029/2020GL088776>
- Maher, N., Lehner, F., & Marotzke, J. (2020). Quantifying the role of internal variability in the temperature we expect to observe in the coming decades. *Environmental Research Letters*, *15*(5), 054014. <https://doi.org/10.1088/1748-9326/ab7d02>
- Mann, M. E., & Rutherford, S. (2002). Climate reconstruction using Pseudoproxies. *Geophysical Research Letters*, *29*(10), 139–139-4. <https://doi.org/10.1029/2001GL014554>
- Mann, M. E., Rutherford, S., Wahl, E., & Ammann, C. (2005). Testing the fidelity of methods used in proxy-based reconstructions of past climate. *Journal of Climate*, *18*(20), 4097–4107. <https://doi.org/10.1175/JCLI3564.1>
- Mann, M. E., Rutherford, S., Wahl, E., & Ammann, C. (2007). Robustness of proxy-based climate field reconstruction methods. *Journal of Geophysical Research*, *112*(D12). <https://doi.org/10.1029/2006JD008272>
- Mann, M. E., Zhang, Z., Rutherford, S., Bradley, R. S., Hughes, M. K., Shindell, D., et al. (2009). Global signatures and dynamical origins of the little ice age and medieval climate anomaly. *Science*, *326*(5957), 1256–1260. <https://doi.org/10.1126/science.1177303>
- Matalas, N. C. (1962). Statistical properties of tree ring data. *International Association of Scientific Hydrology. Bulletin*, *7*(2), 39–47. <https://doi.org/10.1080/02626666209493254>
- McPartland, M. Y. (2024). EarthSystemDiagnostics/McPartland_etal_2024_DendroSNR: v1.1 (Version v1.1) [Software]. *Zenodo*. <https://doi.org/10.5281/zenodo.10822165>
- McPartland, M. Y., St. George, S., Pederson, G. T., & Anchukaitis, K. J. (2020). Does signal-free detrending increase chronology coherence in large tree-ring networks? *Dendrochronologia*, *63*, 125755. <https://doi.org/10.1016/j.dendro.2020.125755>
- Meko, D. M. (1981). Applications of Box-Jenkins methods of time series analysis to the reconstruction of drought from tree rings. Retrieved from <https://repository.arizona.edu/handle/10150/191062>
- Melvin, T. M., & Briffa, K. R. (2008). A “signal-free” approach to dendroclimatic standardisation. *Dendrochronologia*, *26*(2), 71–86. <https://doi.org/10.1016/j.dendro.2007.12.001>
- Melvin, T. M., & Briffa, K. R. (2014a). CRUST: Software for the implementation of Regional Chronology Standardisation: Part 1. Signal-Free RCS. *Dendrochronologia*, *32*(1), 7–20. <https://doi.org/10.1016/j.dendro.2013.06.002>
- Melvin, T. M., & Briffa, K. R. (2014b). CRUST: Software for the implementation of Regional Chronology Standardisation: Part 2. Further RCS options and recommendations. *Dendrochronologia*, *32*(4), 343–356. <https://doi.org/10.1016/j.dendro.2014.07.008>
- Morice, C. P., Kennedy, J. J., Rayner, N. A., Winn, J. P., Hogan, E., Killick, R. E., et al. (2021). An updated assessment of near-surface temperature change from 1850: The HadCRUT5 data set. *Journal of Geophysical Research: Atmospheres*, *126*(3), e2019JD032361. <https://doi.org/10.1029/2019JD032361>
- Münch, T., & Laepple, T. (2018). What climate signal is contained in decadal- to centennial-scale isotope variations from Antarctic ice cores? *Climate of the Past*, *14*(12), 2053–2070. <https://doi.org/10.5194/cp-14-2053-2018>
- Nelson, W. A. (2008). Statistical methods. In S. E. Jørgensen & B. D. Fath (Eds.), *Encyclopedia of ecology* (pp. 3350–3362). Academic Press. <https://doi.org/10.1016/B978-008045405-4.00661-3>
- Neukom, R., Steiger, N., Gómez-Navarro, J. J., Wang, J., & Werner, J. P. (2019). No evidence for globally coherent warm and cold periods over the preindustrial Common Era. *Nature*, *571*(7766), 550–554. <https://doi.org/10.1038/s41586-019-1401-2>
- North, G. R., Wang, J., & Genton, M. G. (2011). Correlation models for temperature fields. *Journal of Climate*, *24*(22), 5850–5862. <https://doi.org/10.1175/2011JCLI4199.1>
- PAGES 2k Consortium, Ahmed, M., Anchukaitis, K. J., Asrat, A., Borgeonkar, H. P., Braida, M., et al. (2013). Continental-scale temperature variability during the past two millennia. *Nature Geoscience*, *6*(5), 339–346. <https://doi.org/10.1038/ngeo1797>
- PAGES 2k Consortium, Emile-Geay, J., McKay, N. P., Kaufman, D. S., von Gunten, L., Wang, J., et al. (2017). A global multiproxy database for temperature reconstructions of the Common Era. *Scientific Data*, *4*(1), 170088. <https://doi.org/10.1038/sdata.2017.88>
- Pederson, N., Dyer, J. M., McEwan, R. W., Hessler, A. E., Mock, C. J., Orwig, D. A., et al. (2014). The legacy of episodic climatic events in shaping temperate, broadleaf forests. *Ecological Monographs*, *84*(4), 599–620. <https://doi.org/10.1890/13-1025.1>
- Rydval, M., Druckenbrod, D., Anchukaitis, K. J., & Wilson, R. (2016). Detection and removal of disturbance trends in tree-ring series for dendroclimatology. *Canadian Journal of Forest Research*, *46*(3), 387–401. <https://doi.org/10.1139/cjfr-2015-0366>
- Smerdon, J. E. (2012). Climate models as a test bed for climate reconstruction methods: Pseudoproxy experiments. *WIREs Climate Change*, *3*(1), 63–77. <https://doi.org/10.1002/wcc.149>
- Speer, J. H. (2010). *Fundamentals of tree-ring research*. University of Arizona Press.
- Steiger, N. J., Hakim, G. J., Steig, E. J., Battisti, D. S., & Roe, G. H. (2014). Assimilation of time-averaged pseudoproxies for climate reconstruction. *Journal of Climate*, *27*(1), 426–441. <https://doi.org/10.1175/JCLI-D-12-00693.1>

- St. George, S., & Ault, T. R. (2014). The imprint of climate within Northern Hemisphere trees. *Quaternary Science Reviews*, 89, 1–4. <https://doi.org/10.1016/j.quascirev.2014.01.007>
- Tardif, R., Hakim, G. J., Perkins, W. A., Horlick, K. A., Erb, M. P., Emile-Geay, J., et al. (2019). Last Millennium Reanalysis with an expanded proxy database and seasonal proxy modeling. *Climate of the Past*, 15(4), 1251–1273. <https://doi.org/10.5194/cp-15-1251-2019>
- Thomson, D. J. (1982). Spectrum estimation and harmonic analysis. *Proceedings of the IEEE*, 70(9), 1055–1096. <https://doi.org/10.1109/PROC.1982.12433>
- von Storch, H., Zorita, E., & González-Rouco, F. (2009). Assessment of three temperature reconstruction methods in the virtual reality of a climate simulation. *International Journal of Earth Sciences*, 98(1), 67–82. <https://doi.org/10.1007/s00531-008-0349-5>
- von Storch, H., Zorita, E., Jones, J. M., Dimitriev, Y., González-Rouco, F., & Tett, S. F. B. (2004). Reconstructing past climate from noisy data. *Science*, 306(5696), 679–682. <https://doi.org/10.1126/science.1096109>
- Wilson, R., Anchukaitis, K., Briffa, K. R., Büntgen, U., Cook, E., D'Arrigo, R., et al. (2016). Last millennium northern hemisphere summer temperatures from tree rings: Part I: The long term context. *Quaternary Science Reviews*, 134, 1–18. <https://doi.org/10.1016/j.quascirev.2015.12.005>
- Zhang, H., Yuan, N., Esper, J., Werner, J. P., Xoplaki, E., Büntgen, U., et al. (2015). Modified climate with long term memory in tree ring proxies. *Environmental Research Letters*, 10(8), 084020. <https://doi.org/10.1088/1748-9326/10/8/084020>
- Zhu, F., Emile-Geay, J., Anchukaitis, K. J., McKay, N. P., Stevenson, S., & Meng, Z. (2023). A pseudoproxy emulation of the PAGES 2k database using a hierarchy of proxy system models. *Scientific Data*, 10(1), 624. <https://doi.org/10.1038/s41597-023-02489-1>
- Zhu, F., Emile-Geay, J., Hakim, G. J., King, J., & Anchukaitis, K. J. (2020). Resolving the differences in the simulated and reconstructed temperature response to volcanism. *Geophysical Research Letters*, 47(8), e2019GL086908. <https://doi.org/10.1029/2019GL086908>
- Zhu, F., Emile-Geay, J., McKay, N. P., Hakim, G. J., Khider, D., Ault, T. R., et al. (2019). Climate models can correctly simulate the continuum of global-average temperature variability. *Proceedings of the National Academy of Sciences*, 116(18), 8728–8733. <https://doi.org/10.1073/pnas.1809959116>